



## Special Feature: Novel Catalytic Approach

Research Report

### Application of Non-thermal Plasma and Ozone for Advanced Automotive Exhaust Aftertreatment under Lean-burn Conditions

Yoshihiko Itoh

Report received on Jan. 12, 2016

**■ABSTRACT■** The oxidation of particulate matter (PM) with ozone, and the non-thermal plasma it was produced with, and by plasma assisted catalysis (PAC), was evaluated as an aftertreatment for diesel engine exhaust. The use of ozone resulted in a high oxidation rate of the granular carbon at low temperatures. However, thermal decomposition of the ozone and reactions with other gas components, especially NO, decreased the oxidation rate. These effects can be investigated with the Arrhenius equation. PM collected from a diesel engine's exhaust with a diesel particulate filter showed a similar oxidizing rate to the carbon. A high NO<sub>x</sub> reduction performance and a wide operating temperature window under transient temperature conditions were achieved with the multi-stage catalyst with PAC under lean-burn conditions. These results show that non-thermal plasma and ozone are suitable for the aftertreatment of diesel engine exhaust.

**■KEYWORDS■** Non-thermal Plasma, Catalyst, NO<sub>x</sub> Reduction, Hydrocarbon, Aftertreatment, Lean-burn Conditions, Diesel Engine, Particulate Matter, Ozone, Oxidation

#### 1. Introduction

Diesel engines have been extensively used as power sources to achieve improved fuel economy or low CO<sub>2</sub> emissions; however, these engines have problems regarding particulate matter (PM) and NO<sub>x</sub> emissions. Regarding the problem with PM emissions, diesel particulate filters (DPFs) used to collect PM require periodic regeneration by oxidation of accumulated PM to avoid a decrease in the engine performance due to an increase in exhaust back pressure. Regeneration can be conducted by increasing the exhaust gas temperature with additional fuel injection or with the use of external heaters on the DPF, which leads to increased fuel consumption or additional electric power requirements. PM-oxidizing catalysts and oxidation methods with NO<sub>2</sub> have been developed for DPF regeneration.<sup>(1)</sup> However, the performance of these processes is inadequate because operation is limited to the high temperature region. For the problem with NO<sub>x</sub> emissions, conventional 3-way catalysts are ineffective for NO<sub>x</sub> reduction under lean-burn conditions; therefore, NH<sub>3</sub>-selective catalytic reduction (NH<sub>3</sub>-SCR)<sup>(2)</sup> or NO<sub>x</sub> storage reduction (NSR)<sup>(3)</sup> catalysts have been used for these purposes. However, additional reagents or complicated operation schemes are required for these processes.

Hydrocarbon-selective catalytic reduction (HC-SCR) has also been developed for NO<sub>x</sub> reduction<sup>(4,5)</sup> because of its simplicity, but it also has problems, such as low NO<sub>x</sub> conversion and a narrow operating temperature range.

It was recently reported that non-thermal plasma is effective for PM oxidation<sup>(6,7)</sup> and HC-SCR in the form of plasma-assisted catalysis (PAC).<sup>(8-10)</sup> Aldehydes are also produced by partial oxidation of alkene with ozone,<sup>(11)</sup> which is typically generated by non-thermal plasma.<sup>(12)</sup> Ozone is generally used to treat decomposition odors or for the inactivation of viruses and bacteria because it has greater chemical activity than Cl<sub>2</sub> and H<sub>2</sub>O<sub>2</sub>, and decomposes easily to non-toxic oxygen. Ozone has also been reported to have a high performance for PM oxidation.<sup>(13,14)</sup> A small diesel engine with an AC generator as a load was used with DPF regeneration by ozone injection into the upstream.<sup>(13)</sup> Thermogravimetric analysis (TGA) was used to experimentally compare PM oxidation by O<sub>2</sub> and NO<sub>2</sub>.<sup>(14)</sup> This work was extended to reflect the actual diesel exhaust obtained from large-scale automotive diesel engines and PM oxidation was investigated in detail using ozone under conditions that correspond to actual diesel exhaust.<sup>(15)</sup>

As reported previously, the reaction mechanism over  $\gamma$ -alumina with PAC is considered to involve

(1) the reaction of partially oxidized HCs and  $\text{NO}_2$  on the acid sites of  $\gamma$ -alumina and the promotion of their adsorption onto the alumina, and (2) promotion of the slow reaction step for the formation of  $\text{NO}_2$  and partially oxidized HCs by non-thermal plasma.<sup>(16)</sup> To solve the problems of HC-SCR, low  $\text{NO}_x$  conversion and the narrow operation temperature window, a combination of the catalysts with PAC is considered to be more effective.

In this paper, we report on low temperature PM oxidation using ozone with quantitative evaluation by Arrhenius equations, and  $\text{NO}_x$  reduction by PAC as an application of non-thermal plasma for the potential aftertreatment of diesel engine exhaust.

## 2. Experimental

### 2.1 PM Oxidation with Ozone

**Figure 1** shows the experimental apparatus used for PM oxidation with ozone. The PM oxidation performance of ozone was investigated with respect to (1) the fundamental oxidation performance of ozone, where granular carbon (Kishida Chemical Co. Ltd., 1-1.7 mm pellets, reagent grade, 3 mL) was used as a model PM with crushed quartz (1-1.7 mm pellets, 7 mL), (2) application to PM collected with a DPF (30 mm diameter, length 50 mm, 0.155 cells/ $\text{mm}^2$ ) in the exhaust system of an automotive diesel engine (2 L displacement, 4-cylinder, direct injection, operated with a torque of 30 Nm at 2000 rpm). The amount of

PM collected from the DPF was 80 mg. The DPF was calcined at 573 K for 1 h in air after PM collection to remove the soluble organic fraction (SOF).

A gas generator was used to mix  $\text{N}_2$ ,  $\text{H}_2\text{O}$ ,  $\text{NO}$ ,  $\text{NO}_2$ ,  $\text{C}_3\text{H}_6$ , and  $\text{CO}$  as the simulated diesel exhaust gas, to which ozone was then added from an ozonizer (Nippon Ozone Co. Ltd., IO-1A6). The oxidation rates of carbon and PM were evaluated from measurements of the  $\text{CO}$  and  $\text{CO}_2$  concentrations using a non-dispersive infrared gas analyzer (Shimadzu Corp., GCT-7000). Ozone and other gas components were measured using an ozone monitor (Ebara Jitsugyo, Co. Ltd., PG-620 PA) and an exhaust gas analyzer (Horiba, Ltd., MEXA-9100D), respectively. **Table 1** shows the experimental conditions used for PM and carbon oxidation (PM and C ox.), the thermal decomposition of ozone ( $\text{O}_3$  decomp.), and the reaction of ozone with other gas components ( $\text{O}_3$  react.).

### 2.2 $\text{NO}_x$ Reduction with PAC

The experimental apparatus for PAC is shown in **Fig. 2**. The plasma reactor and catalyst reactor were set in separate furnaces in the line of the gas flow. For the generation of non-thermal plasma, dielectric barrier discharge was performed using a pulsed high-voltage power supply with a rotary spark-gap switch, a peak voltage of 10-15 kV, and a frequency of 230 Hz.  $\gamma$ -alumina, alkali or alkaline earth metal (Li, Na, K, Mg, Ca, Sr, and Ba)-loaded H-ZSM-5, Pt/ $\gamma$ -alumina (Pt/alumina) and In/ $\gamma$ -alumina (In/alumina) catalysts

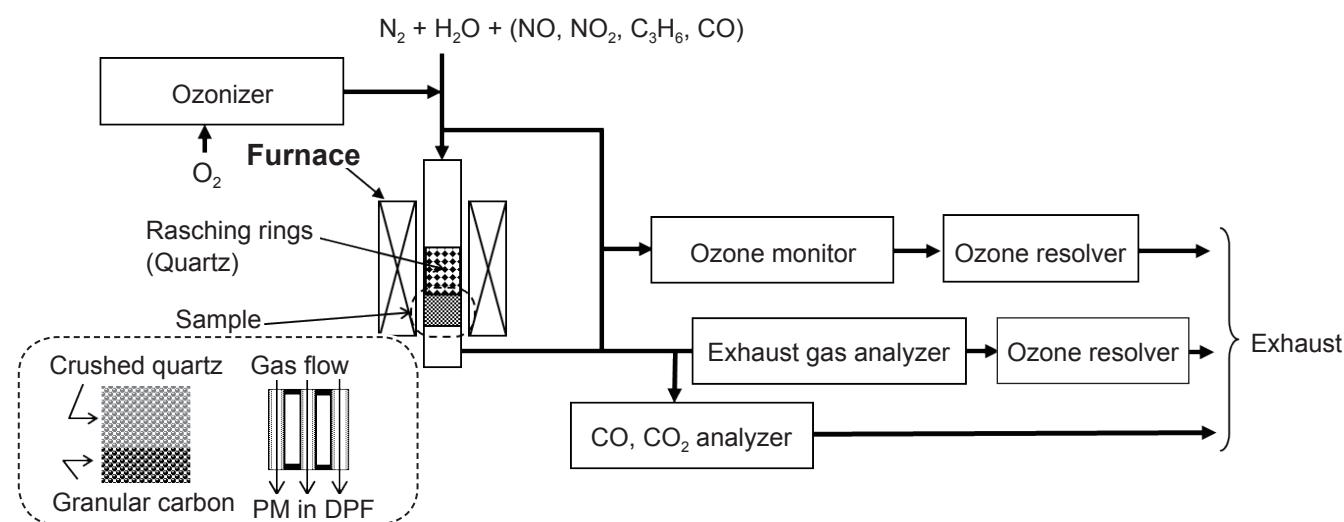


**Fig. 1** Experimental apparatus for PM oxidation with ozone.

were also used for comparison, where powders of these catalysts were formed into 1-3 mm diameter pellets.

The inlet gas composition was selected to simulate diesel exhaust. The inlet gas and outlet gas of the reactors were measured using the exhaust gas analyzer system.  $\text{NO}_x$  conversion was measured by the following methods: (1) averaging  $\text{NO}_x$  conversion under cooling conditions, (2) temperature dependence of  $\text{NO}_x$  conversion under steady-state conditions,

(3)  $\text{NO}_x$  conversion to simulate the transition states of the automobile exhaust. The temperature profile for these procedures simulated that of diesel engine exhaust produced in the Japanese 10-15 mode cycle using the fastest temperature ramp (40 K/min) available with this apparatus. The experimental conditions for PAC are shown in **Table 2**. The details for catalyst preparation have been described elsewhere.<sup>(16)</sup>

**Table 1** Inlet gas conditions for PM oxidation using ozone.

	Concentration								Inlet gas temperature (K)	Total gas flow rate (L/min)
	$\text{O}_3$ (ppm)	NO (ppm)	$\text{NO}_2$ (ppm)	$\text{C}_3\text{H}_6$ (ppm C)	CO (ppm)	$\text{O}_2$ (%)	$\text{H}_2\text{O}$ (%)	$\text{N}_2$		
PM and Cox.	0-930	0-550	0-550	-	-	10	3	Balance	298-573 (steady-state)	10
$\text{O}_3$ decomp.	0-930	-	-	-	-	10	3	Balance	298-573 (heating 10 K/min)	10
$\text{O}_3$ react.	400-930	0-550	0-550	0-1000	0-1000	10	3	Balance	298-573 (steady-state)	10

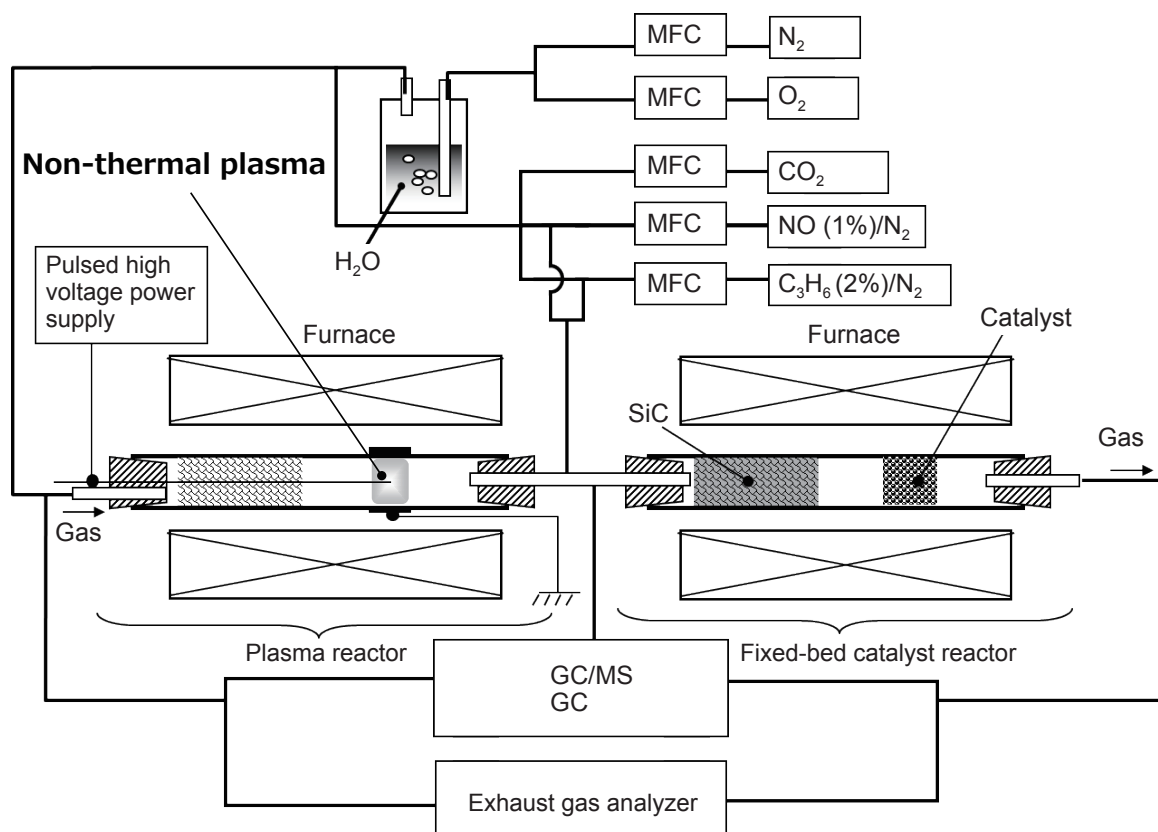


**Fig. 2** Experimental apparatus used for PAC.

### 3. Results and Discussion

#### 3.1 PM Oxidation with Ozone

##### 3.1.1 Fundamental Study of Carbon Oxidation Using Ozone

To evaluate the performance of ozone for PM oxidation, the temperature dependence of the carbon oxidation rate was first investigated quantitatively with respect to the Arrhenius behavior. Both carbon oxidation by ozone and the thermal decomposition of ozone increases with temperature. Therefore, the amount of thermally decomposed ozone was evaluated without carbon in the reactor. Equation (1) describes the amount of ozone decomposed with respect to the ambient temperature:

$$C_{O_3, T} = 1000C_{O_3, \text{supp.}}^{1.22} e^{-4440/T}, \quad (1)$$

$C_{O_3, T}$ : amount of thermally decomposed ozone (mmol/h),

$C_{O_3, \text{supp.}}$ : amount of supplied ozone (mmol/h),

$T$ : temperature (K).

Equation (2) describes the carbon oxidation rate, including the effect of thermally decomposed ozone obtained from Eq. (1):

$$r_T = 79.883(C_{O_3, \text{supp.}} - C_{O_3, T})e^{-2088.5/T}, \quad (2)$$

$r_T$ : carbon oxidation rate with thermal decomposition of ozone (mmol/h).

The experimentally measured results are shown with the calculated results in Fig. 3. Figure 3(a) shows the temperature dependence of the ozone decomposition rate with that calculated using Eq. (1). The measured results are consistent with those calculated using Eq. (1) for various amounts of ozone at the inlet. Figure 3(b) shows the temperature dependence of the carbon oxidation rate using ozone with that calculated from Eq. (2) with the amount of thermally decomposed ozone obtained from Eq. (1). When compared with the measured values, Eq. (2) describes the decrease in the carbon oxidation rate with good accuracy and consistency at high temperatures exceeding 523 K up to 573 K. Thus, the carbon oxidation rate using ozone can be precisely described by Arrhenius equations for the evaluation of thermally decomposed ozone at the ambient temperature.

These results show that the amount of residual ozone after reaction with the other gas components determines the carbon oxidation rate and suggests that the reaction of highly reactive gas components with ozone causes a decrease in the carbon oxidation rate by decreasing the amount of ozone for carbon oxidation. The rate constants for reaction of the various gas

**Table 2** Experimental conditions for PAC.

Inlet gas	NO	200 ppm	
	O <sub>2</sub>	10%	
	C <sub>3</sub> H <sub>6</sub>	3000 ppm C	
	CO <sub>2</sub>	4%	6.7%
	H <sub>2</sub> O	2%	5%
	N <sub>2</sub>	Balance	
Catalyst	Pellet		
Flow rate	2 L/min		5 L/min
Space velocity	60000 h <sup>-1</sup>		30000 h <sup>-1</sup>
Temperature	673-423 K, cooling, 30K/min	323-573 K, steady-state	773-423 K, cooling 40 K/min 423 k, hold, 1 min 423-773 K, heating 40 K/min
Voltage (Specific energy)	12.5 kV (30 J/L)		14.5 kV (16 J/L)

components with ozone have been reported to follow the order  $\text{NO} > \text{NO}_2 > \text{C}_3\text{H}_6 > \text{SO}_2 > \text{C}_3\text{H}_8 > \text{CH}_4 > \text{CO}$ .<sup>(17-22)</sup> Therefore, the effect of ozone reaction with other gas components was evaluated, and the results are shown in Fig. 4 as the ozone residual ratio, i.e., the ratio of the residual ozone concentration to the inlet ozone concentration, and the ozone/NO reaction ratio, i.e., the ratio of the reacted ozone concentration to the inlet NO concentration. Figure 4(a) shows the ozone residual ratio containing NO, NO<sub>2</sub>, C<sub>3</sub>H<sub>6</sub>, and CO, where no ozone remains with the NO. On the other hand, there is no reaction between CO and ozone. The reactivity with ozone was determined to be in the order of  $\text{NO} > \text{NO}_2 > \text{C}_3\text{H}_6 > \text{CO}$ , which is consistent with the previously reported results.<sup>(17-22)</sup> Thus, the carbon oxidation rate would be significantly decreased by ozone consumption through reaction with NO. The amount of ozone consumption through reaction

with NO is defined as the ozone/NO reaction ratio, described by Eq. (3):

$$k_{\text{O}_3, \text{NO}} = 0.65316 e^{0.00286T}, \quad (3)$$

$k_{\text{O}_3, \text{NO}}$ : ozone/NO reaction ratio.

Figure 4(b) shows the results for the ozone/NO reaction ratio, where the calculated ozone/NO reaction ratio is reasonably consistent with the measured ratio. These ratios always exceeded 1 and increased with the temperature, which could suggest the formation of highly oxidized nitrates, such as NO<sub>3</sub> and N<sub>2</sub>O<sub>5</sub>, in addition to NO<sub>2</sub>.<sup>(23)</sup> Consequently, the amount of ozone reacted with NO can be described by Eq. (4), which includes Eq. (3):

$$C_{\text{O}_3, \text{NO}} = k_{\text{O}_3, \text{NO}} C_{\text{NO}}, \quad (4)$$

$C_{\text{O}_3, \text{NO}}$ : amount of ozone reacted with NO (mmol/h),  
 $C_{\text{NO}}$ : amount of inlet NO (mmol/h).

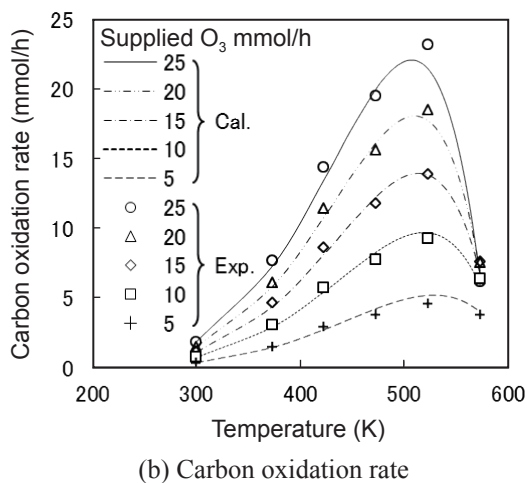
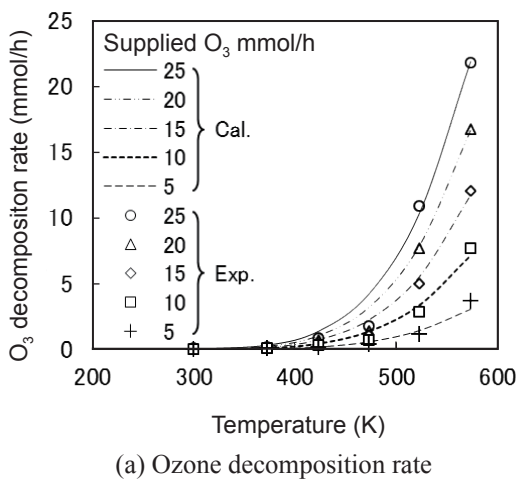


Fig. 3 Experimental and calculated temperature dependence of ozone decomposition and carbon oxidation rates.

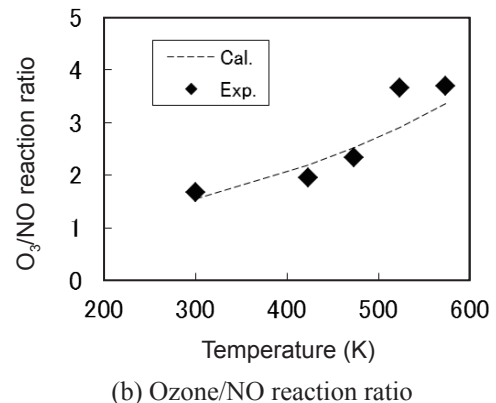
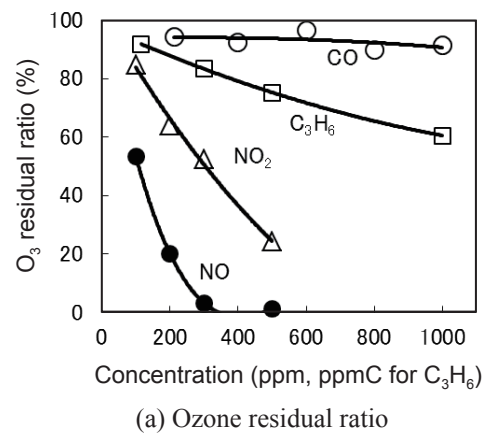


Fig. 4 Effect of ozone reaction with other gas components.

These results are summarized as follows: the ozone reacts with NO prior to thermal decomposition; therefore, the ozone-NO reaction would consume ozone at the inlet before thermal decomposition occurs. The amount of thermally decomposed ozone and that reacted with NO is described by Eq. (5). The carbon oxidation rate when using ozone containing NO can thus be described by Eq. (6), which is determined using Eqs. (1) to (5). **Figure 5** shows the carbon oxidation rate with ozone containing NO, both the measured rates and that calculated using Eq. (6). The calculated rate is consistent with the experimental rate for various amounts of supplied ozone, from 15 to 25 mmol/h (560 to 930 ppm) at 423 K. In conclusion, the carbon oxidation rate with ozone containing NO at ambient temperature could be successfully calculated using Eq. (6).

$$C_{O_3, T, NO} = 1000 (C_{O_3, \text{supp.}} - C_{O_3, NO})^{1.22} e^{-4440/T}, \quad (5)$$

$$r_{T, NO} = 79.883(C_{O_3, \text{supp.}} - C_{O_3, NO} - C_{O_3, T, NO})e^{-2088.5/T}, \quad (6)$$

$C_{O_3, T, NO}$ : amount of thermally decomposed ozone and that reacted with NO (mmol/h),

$r_{T, NO}$ : oxidation rate with thermal decomposition of ozone and reaction of ozone with NO (mmol/h).

Water vapor was included in the inlet gas by the addition of ion-exchanged water to the inlet  $N_2$  gas for simulation of the exhaust gas; however, water was observed to have no effect on the carbon oxidation rate with ozone.

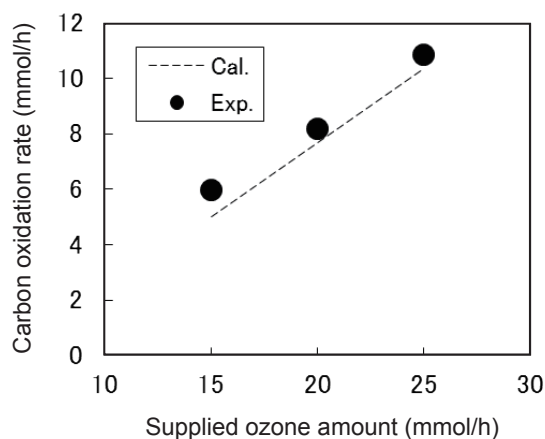
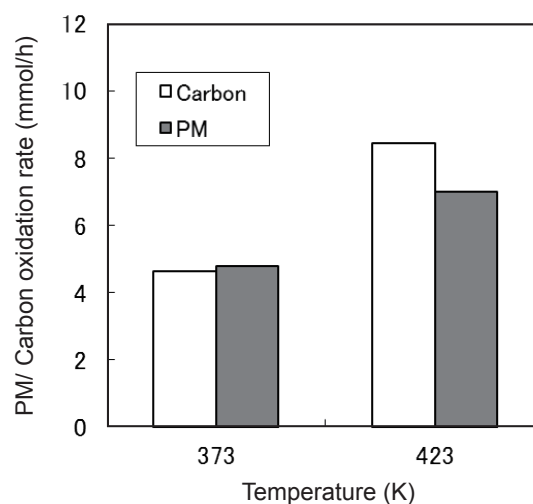


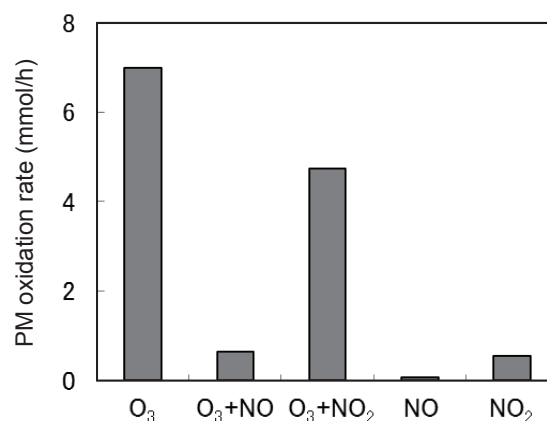
**Fig. 5** Experimental and calculated carbon oxidation rates using ozone containing NO.

### 3. 1. 2 PM Oxidation with Ozone for Practical Application

PM oxidation with ozone was evaluated for practical applications using PM collected from actual DPFs. **Figure 6(a)** shows the PM and carbon oxidation rate obtained with ozone. There was no significant difference in the oxidation rates for PM and carbon at 373 and 423 K, which confirms that the carbon material used in this study was appropriate as a model PM for oxidation with ozone. Figure 6(b) shows the PM oxidation rates with various gas components at 423 K. The presence of NO significantly decreased the PM oxidation rate with ozone. However, in the presence of  $NO_2$ , the decrease of the PM oxidation rate with ozone was less than that for NO. Extremely low PM oxidation rates were obtained at 423 K in



(a) PM and carbon oxidation rates using ozone



(b) PM oxidation rate with various gas components

**Fig. 6** PM and carbon oxidation rates using ozone.

the presence of only NO and NO<sub>2</sub> without ozone. Thus, under the low-temperature conditions similar to those used in this study, the performance for PM oxidation using NO<sub>2</sub><sup>(1)</sup> would be insufficient because all of the supplied ozone reacts to completely oxidize NO to NO<sub>2</sub>. Consequently, PM oxidation using ozone containing NO showed a similar oxidation rate to that using ozone containing only NO<sub>2</sub>.

In contrast, a much higher PM oxidation rate with ozone was achieved than that reported previously from TGA measurements,<sup>(14)</sup> where the large volume of the reaction chamber relative to the size of the PM sample for TGA analysis resulted in overestimation of the thermal decomposition of ozone. This was probably due to the low contact area of PM to the reaction gas.

In conclusion, the conditions for the supply of ozone could be optimized for PM oxidation according to the calculations performed in this study. It was confirmed that PM could be effectively oxidized by ozone, although countermeasures to address the decrease in the amount of ozone available due to reaction with NO are necessary, such as NO reduction or oxidation to NO<sub>2</sub> prior to ozone supply or intermittent supply of high ozone concentration relative to the NO concentration.

### 3.2 NO<sub>x</sub> Reduction under Lean-burn Conditions with PAC

**Figure 7** shows the average NO<sub>x</sub> conversion for the various catalysts from 673 to 423 K, with and without PAC. The NO<sub>x</sub> reduction activities of  $\gamma$ -alumina and the alkali or alkaline earth metal-loaded ZSM-5 catalysts are significantly promoted with PAC and achieve higher performance compared to conventional HC-SCR catalysts such as Pt/alumina and Cu-ZSM-5.

During the Japanese 10-15 mode cycle, the temperature of the exhaust gas for automotive diesel engines generally varies between 423 and 623 K. However, catalysts that cover this temperature range (temperature window) have not yet been developed. To solve this problem, a multi-stage catalyst that consists of several catalysts with different temperature windows was examined. Although such a catalyst has been reported in a similar study for this purpose,<sup>(10)</sup> the performance of the catalyst was inadequate. Therefore, a newly discovered In/alumina catalyst was applied, and the experimental apparatus was operated with a more rapid temperature change, close to that of an actual automotive exhaust system.

**Figure 8** shows the temperature dependence of NO<sub>x</sub> conversion for  $\gamma$ -alumina, In/alumina, Na/ZSM-5, and Pt/alumina with PAC. The temperature for maximum NO<sub>x</sub> conversion over  $\gamma$ -alumina was ca. 773 K, which exceeded the exhaust temperature range for the Japanese 10-15 mode cycle. In contrast, that for In/alumina was ca. 573 K and the temperature window covered almost the entire temperature range for the 10-15 mode cycle. The temperature windows for NO<sub>x</sub> reduction (> 40% NO<sub>x</sub> conversion) were as follows: 423-573 K for Pt/alumina and 473-673 K for both In/alumina and Na/ZSM-5. In addition, Na/ZSM-5 exhibits adsorption ability for HC and NO<sub>2</sub> at 473 K,<sup>(9)</sup> and Pt/alumina can be used as an oxidizing catalyst for HC and CO conversion. Thus, In/alumina, Na/ZSM-5, and Pt/alumina were adopted for the multi-stage catalyst to achieve high NO<sub>x</sub> and HC conversion with a wide operation temperature window.

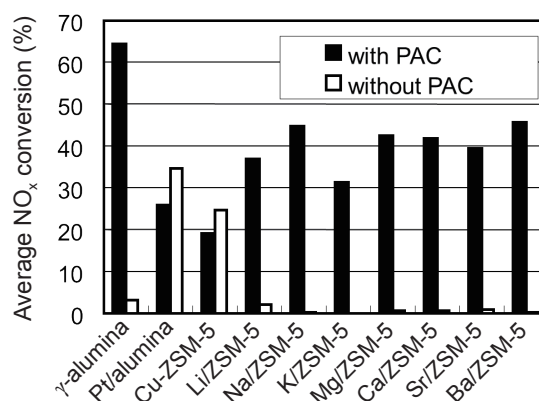


**Fig. 7** Average NO<sub>x</sub> conversion with and without PAC.

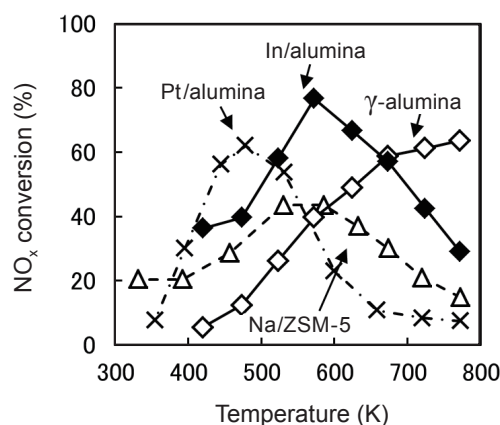


**Fig. 8** Temperature dependence of NO<sub>x</sub> conversion over  $\gamma$ -alumina, In/alumina, Na/ZSM-5 and Pt/alumina with PAC.

To optimize the catalyst performance, these catalysts were set in the reactor from upstream to downstream of the gas flow in the following order: Na/ZSM-5, In/alumina, and Pt/alumina. The functions of each catalyst are described as follows: (1) Na/ZSM-5 (upstream) adsorbs  $\text{NO}_x$  and HC at lower temperatures than the other catalysts, (2) In/alumina (middle) reduces  $\text{NO}_x$  including  $\text{NO}_x$  released from Na/ZSM-5 at higher temperatures by HC-SCR, and (3) Pt/alumina (downstream) oxidizes residual HC and CO. The results for the multi-stage catalyst are shown in **Fig. 9**. A high  $\text{NO}_x$  reduction activity and a wide operation temperature window were obtained. The  $\text{NO}_x$  conversion for the heating section was lower than that for the cooling section, which is attributed to the adsorption of  $\text{NO}_x$  and HC on the catalysts. Two peaks of  $\text{NO}_x$  conversion were observed for the cooling section; the first peak was attributed to  $\text{NO}_x$  reduction by In/alumina and Na/ZSM-5, and the second to Pt/alumina, due to the temperature dependence of  $\text{NO}_x$  conversion over these catalysts determined from Fig. 8. In contrast,  $\text{NO}_x$  conversion in the heating section was decreased by the desorption of  $\text{NO}_x$  from the catalysts. In addition, high HC conversion was obtained at temperatures exceeding 473 K. The CO emission with this multi-stage catalyst was below the detection limit of 5 ppm (data not shown). Consequently, the combination of this multi-stage catalyst with PAC could extend the operating temperature range compared to that using a single catalyst with PAC, and high  $\text{NO}_x$  reduction activity could be achieved at lower temperatures ( $< 423$  K) than that with  $\text{NH}_3$ -SCR<sup>(2)</sup> and NSR<sup>(3)</sup> catalysts. These results confirm the multi-stage catalyst as an effective aftertreatment system under

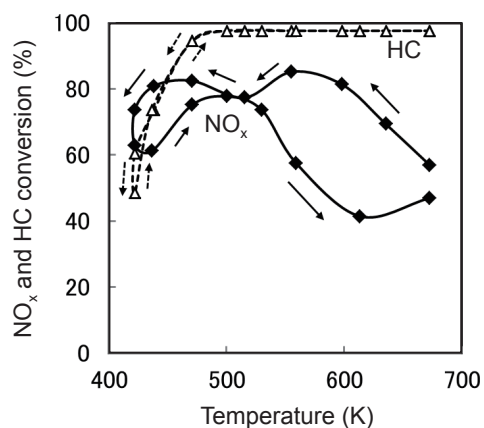


**Fig. 9**  $\text{NO}_x$  and HC conversion over multi-stage catalyst with PAC.

lean-burn conditions with high  $\text{NO}_x$  reduction performance and a wide operation range for transient temperature conditions.

#### 4. Conclusions

The use of ozone, and the non-thermal plasma it was produced with, for the aftertreatment of diesel exhaust was investigated. Low-temperature PM oxidation occurred in DPFs with the addition of ozone to the exhaust gas, thus enabling the regeneration of DPFs without the need for heating by increasing the exhaust gas temperature or by the use of electric heaters. However, the inlet gas containing NO significantly decreased the PM oxidation rate by NO-ozone reaction. The results of this study would also provide a precise prediction of the PM oxidation rate by ozone under actual exhaust conditions. Thus such a quantitative approach is necessary to optimize the performance for PM oxidation by ozone in practical applications. On the other hand,  $\text{NO}_x$  reduction by HC-SCR with PAC confirmed that non-thermal plasma oxidized NO and HC can enhance the HC-SCR reaction and that high  $\text{NO}_x$  conversion and a wide operating temperature range can be achieved by a combination of appropriate catalysts under the oxidative conditions examined. Consequently, the application of non-thermal plasma and its product of ozone is expected to be a promising method for the aftertreatment of diesel engine exhaust.

In addition, for both PAC and ozone generation, the aftertreatment system could be simplified through the use of similar high-voltage power supplies, or through the shared use of a single high-voltage power supply. The application of both PAC for  $\text{NO}_x$  reduction and ozone for PM oxidation are thus promising for the aftertreatment of diesel engine exhaust that cannot be achieved by conventional methods.

#### Acknowledgments

The author thanks Dr. H. Hirata, Mr. M. Kakinohana and Mr. M. Ibe (Toyota Motor Co. Ltd.) for PM sampling and discussion regarding the experiments.

#### References

- (1) Chatterjee, S. et al., "Emission Reduction in On-road Heavy Duty Diesel Applications with the Continuously Regenerating Technology (CRT®) Diesel Particulate Filter", *SAE Tech. Pap. Ser.*,



- No. 2001-28-0049 (2001).
- (2) Iwasaki, M., "Selective Catalytic Reduction of NO<sub>x</sub> by Ammonia: Fe/zeolite Catalyst Development and Reaction Analysis", *R&D Review of Toyota CRDL*, Vol. 42, No. 1 (2011), pp. 21-32.
  - (3) Takahashi, N., "NO<sub>x</sub> Storage and Reduction Catalysts for Gasoline-fueled Automotive Exhaust", *R&D Review of Toyota CRDL*, Vol. 42, No. 1 (2011), pp. 9-19.
  - (4) Iwamoto, M. et al., "Performance and Durability of Pt-MFI Zeolite Catalyst for Selective Reduction of Nitrogen Monoxide in Actual Diesel Engine Exhaust", *Appl. Catal. B*, Vol. 5, No. 1-2 (1994), pp. L1-L5.
  - (5) Hamada, H. et al., "Transition Metal-promoted Silica and Alumina Catalysts for the Selective Reduction of Nitrogen Monoxide with Propane", *Appl. Catal.*, Vol. 75, No. 1 (1991), pp. L1-L8.
  - (6) Yao, S. et al., "Oxidation of Activated Carbon and Methane Using a High-frequency Pulsed Plasma Original Research Article", *J. Hazard. Mater.*, Vol. 83, No. 3 (2001), pp. 237-242.
  - (7) Naito, K. et al., "Comprehensive Technological Development of Innovative, Next-generation, Low-pollution Vehicles: Development of PM Removal System for a Diesel Engine Using a Non-thermal Plasma Reactor with Porous Electrodes", *Proc. JSAE Ann. Congr.* (in Japanese), No. 20075740 (2007).
  - (8) Panov, A. G. et al., "Selective Reduction of NO<sub>x</sub> in Oxygen Rich Environments with Plasma-assisted Catalysis: The Role of Plasma and Reactive Intermediates", *SAE Tech. Pap. Ser.*, No. 2001-01-3513 (2001).
  - (9) Ebeling, A. C. et al., "Characterization of Acid Sites in Ion-exchanged and Solid State-exchanged Zeolites", *SAE Tech. Pap. Ser.*, No. 2001-01-3571 (2001).
  - (10) Tonkyn, R. G. et al., "Reduction of NO<sub>x</sub> in Synthetic Diesel Exhaust via Two-step Plasma-catalysis Treatment", *Appl. Catal. B*, Vol. 40, No. 3 (2003), pp. 207-217.
  - (11) Grosjean, D., "Gas-phase Reaction of Ozone with 2-methyl-2-butene: Dicarbonyl Formation from Criegee Biradicals", *Environ. Sci. Technol.*, Vol. 24, No. 9 (1990), pp. 1428-1432.
  - (12) Takaki, K. et al., "Influence of Circuit Parameter on Ozone Synthesis Using Inductive Energy Storage System Pulsed Power Generator", *IEEE Trans. Dielectr. Electr. Insul.*, Vol. 18, No. 5 (2011), pp. 1752-1758.
  - (13) Okubo, M. et al., "Recent Development of Diesel Particulate and NO<sub>x</sub> Reduction Aftertreatment System Using Nonthermal Plasma", *Proc. JSAE Ann. Congr.*, No. 20055437 (2005).
  - (14) Yao, S. et al., "Comprehensive Technological Development of Innovative, Next-generation, Low-pollution Vehicles Basic Study of PM Oxidation Promoted by O<sub>3</sub> and NO<sub>2</sub>", *Proc. JSAE Ann. Congr.* (in Japanese), No. 20075799 (2007).
  - (15) Itoh, Y. et al., "Low-temperature Oxidation of Particulate Matter Using Ozone", *RSC Adv.*, Vol. 4, No. 37 (2014), pp. 19144-19149.
  - (16) Itoh, Y. et al., "NO<sub>x</sub> Reduction under Oxidizing Conditions by Plasma-assisted Catalysis", *R&D Review of Toyota CRDL*, Vol. 41, No. 2 (2006), pp. 49-62.
  - (17) Lippmann, H. H. et al., "The Rate-constant of NO+O<sub>3</sub>-NO<sub>2</sub>+O<sub>2</sub> in the Temperature-range of 283-443 K", *Int. J. Chem. Kinet.*, Vol. 12, No. 8 (1980), pp. 547-554.
  - (18) DeMore, W. B. et al., "Chemical Kinetics and Photochemical Data for Use in Stratospheric Modeling", *JPL Publication*, Vol. 97, No. 4 (1997), pp. 1-266.
  - (19) Greene, C. R. and Atkinson, R., "Rate Constants for the Gas-phase Reactions of O<sub>3</sub> with a Series of Alkenes at 296K±2K", *Int. J. Chem. Kinet.*, Vol. 24, No. 9 (1992), pp. 803-811.
  - (20) Morrissey, R. J. and Schubert, C. C., "The Reactions of Ozone with Propane and Ethane", *Combust. Flame*, Vol. 7 (1963), pp. 263-268.
  - (21) Dilleuth, F. J. et al., "The Reaction of Ozone with Methane", *J. Phys. Chem.*, Vol. 64, No. 10 (1960), pp. 1496-1499.
  - (22) Arin, L. M. and Warneck, P., "Reaction of Ozone with Carbon Monoxide", *J. Phys. Chem.*, Vol. 76, No. 11 (1972), pp. 1514-1516.
  - (23) Graham, R. A. and Johnston, H. S., "The Photochemistry of NO<sub>3</sub> and the Kinetics of the N<sub>2</sub>O<sub>5</sub>-O<sub>3</sub> System", *J. Phys. Chem.*, Vol. 82, No. 3 (1978), pp. 254-268.
- Figs. 1, 3-6 and Table 1  
Reprinted from *RSC Adv.*, Vol. 4, No. 37 (2014), pp. 19144-19149, Itoh, Y. et al., Low-temperature Oxidation of Particulate Matter Using Ozone, © 2014 The Royal Society of Chemistry.
- Figs. 2 and 7  
Reprinted from *R&D Review of Toyota CRDL*, Vol. 41, No. 2 (2006), pp. 49-62, Itoh, Y. et al., NO<sub>x</sub> Reduction under Oxidizing Conditions by Plasma-assisted Catalysis, © 2006 Toyota Central R&D Labs., Inc.

#### Yoshihiko Itoh

Research Field:

- Catalysis & Catalyst Development

Academic Degree: Dr.Eng.

Academic Society:

- Surface Finishing Soc. Jpn.

